Three-dimensional architecture of the Nankai accretionary prism's imbricate thrust zone off Cape Muroto, Japan: Prism reconstruction via en echelon thrust propagation

S. P. S. Gulick,[1] N. L. B. Bangs,[1] T. H. Shipley,[1] Y. Nakamura,[2] G. Moore,[3] and S. Kuramoto[4]

Received 24 June 2003; revised 23 October 2003; accepted 5 November 2003; published 18 February 2004.

[1] A 9 km wide, 92 km long, three-dimensional (3-D) seismic reflection volume acquired off Shikoku Island, Japan, images the seaward portion of the subduction of the Philippine Sea plate at the Nankai Trough and Nankai accretionary prism. Detailed interpretation of the imbricate thrust and protothrust zones, the portions of the prism between the deformation front and the first out-of-sequence thrust, shows a high degree of variability in the thrust faults that all parallel the frontal thrust but are arranged in en echelon patterns along strike and frequently include complications such as piggyback faults and fault splays. Interestingly, the sinuous seafloor morphology of the prism does not accurately reflect the en echelon 3-D architecture of the primary prism thrusts. Seafloor morphology appears to average across several thrusts along strike and is further modified by near-surface thrust splays and backthrusts, suggesting that care must be taken in interpreting seafloor relief in terms of lateral continuity or thrust fault geometry. Subduction of the Kinan seamounts 20 km northeast of the center of the Muroto 3-D volume generated a scallop-shaped embayment in the prism; the rebuilding process appears to influence the northeastern portion of the 3-D volume where a ~625 m landward step in the position of the frontal thrust and numerous changes in prism architecture are observed. These observations imply that accretionary prisms may reattain equilibrium following seamount subduction by lateral en echelon fault propagation into damaged zones that facilitate an increase accretion rate until a laterally continuous deformation front is reestablished. *INDEX TERMS:* 3025 Marine Geology and Geophysics: Marine seismics (0935); 3045 Marine Geology and Geophysics: Seafloor morphology and bottom photography; 3040 Marine Geology and Geophysics: Plate tectonics (8150, 8155, 8157, 8158); 8010 Structural Geology: Fractures and faults; 8015 Structural Geology: Local crustal structure; *KEYWORDS:* Nankai Trough, accretionary prism, en echelon

Citation: Gulick, S. P. S., N. L. B. Bangs, T. H. Shipley, Y. Nakamura, G. Moore, and S. Kuramoto (2004), Three-dimensional architecture of the Nankai accretionary prism's imbricate thrust zone off Cape Muroto, Japan: Prism reconstruction via en echelon thrust propagation, *J. Geophys. Res.*, *109*, B02105, doi:10.1029/2003JB002654.

1. Introduction

[2] The Nankai Trough convergent margin lies offshore southwest Japan where the Philippine Sea plate is subducting at an azimuth of ~305° beneath the Amurian plate at a rate of ~6.55 cm/yr (Figure 1) [*Miyazaki and Heki*, 2001]. Overlying the subducting Philippine Sea plate are the Shikoku Basin sediments that, due to this convergence, are in part subducted beneath and in part accreted to the margin. This accretion of sediments at the Nankai Trough forms the Nankai accretionary prism.

[3] The Nankai accretionary prism off Cape Muroto, Shikoku Island, has been extensively studied through Ocean Drilling Program Legs 131, 190, and 196 [*Mikada et al.*, 2002; *Moore et al.*, 2001b, 2001c; *Taira et al.*, 1991], surficially mapped with SeaBeam and IZANAGI side-scan sonar [*Ashi et al.*, 1989; *Kaiko I Research Group*, 1986], surveyed by numerous submersible and ROV dives [e.g., *Kuramoto et al.*, 2001; *LePichon et al.*, 1987a, 1987b; *Mikada et al.*, 2003], and imaged by a series of seismic reflection and refraction experiments [*Aoki et al.*, 1986, 1982; *Bangs et al.*, 1999; *Kodaira et al.*, 2000; *Leggett et al.*, 1985; *Moore et al.*, 1991; *Moore and Shipley*, 1993; *Moore et al.*, 1990, 2001a; *Nasu et al.*, 1982; *Park et al.*, 1999, 2000; *Tamano et al.*, 1983]. In this paper, we present the results of a portion of a 9 km wide, 92 km long 3-D seismic reflection volume acquired in mid-June to mid-August 1999 [*Bangs et al.*, 1999; *Moore et al.*, 2001a],

[1]Institute for Geophysics, University of Texas at Austin, Austin, Texas, USA.
[2]Ocean Research Institute, University of Tokyo, Tokyo, Japan.
[3]Department of Geology and Geophysics and School of Ocean and Earth Science and Technology, University of Hawai'i, Honolulu, Hawaii, USA.
[4]Institute for Marine Resources and Environment, National Institute of Advanced Industrial Science and Environment, Tsukuba, Japan.

0148-0227/04/2003JB002654$09.00

which is the largest 3-D seismic volume ever collected by academia. The Muroto 3-D volume allows us an unparalleled opportunity to examine the effect of along-strike differences in subduction processes and accommodation of strain.

[4] Accretion along the Nankai margin started occurring in the Cretaceous as demonstrated by the imbricated thrust slices of mélanges and trench turbidites of the Cretaceous-Tertiary Shimanto Belt on Shikoku Island, Japan [*Ohmori et al.*, 1997; *Taira et al.*, 1988; *Taira and Tashihiro*, 1987]. However, accretion at the Nankai Trough was not likely continuous or the prism would be far larger. The current phase of subduction and accretion of the Shikoku Basin section appears to have started in the Pliocene based on the ages of accretionary prism rocks cored during ODP Leg 190 Sites 1175 and 1176 (Figure 1) [*Moore et al.*, 2001c]. An additional tectonic complication to this history of accretion is the subduction of an extinct spreading center delineated by the Kinan Seamounts [*Okino et al.*, 1994]. The subduction of the Kinan Seamounts has resulted in a prominent embayment known as the Tosa Bae embayment (Figure 1) [*Yamazaki and Okamura*, 1989]; beneath and landward of this embayment, seismic reflection and refraction studies have directly observed individual subducting seamounts [*Kodaira et al.*, 2000; *Park et al.*, 1999]. The Muroto 3-D volume crosses the western edge of the Tosa Bae embayment (Figure 1) with its approximate center lying ~20 km from the center of the 3-D volume.

[5] Preliminary interpretation of the 3-D seismic volume divides the accretionary prism along the Muroto Transect into discrete tectonic zones [*Moore et al.*, 2001a]. According to this division, the outermost zone is bounded by the deformation front seaward and the frontal thrust landward and is called the protothrust zone. Approximately 30 km landward of the front thrust is an out-of-sequence thrust (OOST) which generates a prominent seafloor ridge (Figures 1 and 2). The intervening series of thrust faults and seafloor thrust-related ridges are known as the imbricate thrust zone [*Moore et al.*, 1990, 2001b]. Results from ODP Leg 190 show that this part of the prism has been accreted in less than 2 my, suggesting that the prism is rapidly reestablishing the zone of frontal accretion across the Tosa Bae embayment [*Moore et al.*, 2001a].

[6] This paper will examine the structural architecture of the Nankai accretionary prism in the protothrust and imbricate thrust zones. Additional papers are in progress to examine décollement and out-of-sequence thrusting processes. The position of the 3-D volume on the edge of the scalloped-shaped Tosa Bae embayment generated by the subducting Kinan seamounts further allows us to study accretionary prism response to along-strike tectonic influences. While we acknowledge the importance of diffuse lateral shortening mechanisms for prism dewatering and shortening during accretion [e.g., *Byrne et al.*, 1993; *Maltman et al.*, 1993; *Morgan and Karig*, 1995], we suggest an examination of the discrete deformation along fault planes will properly reflect along-strike changes. The primary goals of this paper are to map the along-strike variations of faulting within these zones, to demonstrate the complexity of the thrust faulting, which interestingly, is not fully reflected in the seafloor thrust ridges, to estimate basal frictional strength, to examine deformation mechanisms wherein an accretionary prism reacts to geometric anomalies such as those wrought by subducting seamounts, and to yield insights into the 3-D process of prism rebuilding following seamount subduction.

2. The 3-D Seismic Data Acquisition, Processing, and Interpretation

[7] We acquired the 3-D reflection volume along the corridor known as the Muroto Transect from mid-June to mid-August 1999 using the R/V *Maurice Ewing*. The acquisition parameters included a single 6 km streamer with 160 channels, 14 tuned air guns with a total volume of 4276 cu. in., and a shot spacing of 50 m. We shot 81 separate lines and then filled the volume in with 10 days of reshoots to cover the holes caused by adverse weather, currents, and ship traffic. The resultant survey was a complete 8 × 80 km seismic volume of 151,061 shots and ~500 Gbytes of seismic data.

[8] The 3-D processing of the seismic volume included several steps not needed for conventional academic 2-D processing. Figure 3 shows the basic processing flow used to progress the data from its acquired SEGD field data form to the 3-D time-migrated, depth-converted volume. Following the band-pass filter a series of trace and shot kills were required to remove data acquired during adverse weather, when the source signature was compromised due to the largest or smallest air gun being offline, when the streamer was strongly curved in a turn, and when ship traffic generated too much noise. The reshoots performed filled any holes caused by large areas of shot kills. Sorting and binning of the 3-D shot data into 25 × 50 m CDP bins resulted in a volume that due to streamer feathering was actually 9 × 92.75 km; the variations in streamer feathering however produced an uneven offset distribution in some bins. In order to generate the complete range of shot-receiver offsets, we sorted the edited data into gathers consisting of the common offsets across the survey in the each crossline (the 9 km dimension of the volume). We then performed trace interpolation on these common offset crossline gathers to fill in the complete range of offsets for the entire volume. Following this crossline-offset interpolation, we sorted the data back into the 25 × 50 m 3-D bins and then corrected for normal moveout, stretch muted, and inside muted. To avoid spurious diffractions impacting the imaged strata in the deeper waters, we muted the far offsets of the rough oceanic crust prior to 3-D stacking, poststack deconvolution, and 3-D time migration using our best available velocities. The final volume was converted to depth using our best velocities; the time to depth conversion is appears reasonable based on comparisons with Leg 190 and Leg 196 drilling results.

[9] We completed the interpretation of the faults within the imaged outer accretionary prism using the Geoquest IESX software. We picked the faults by choosing and tracing the strong negative peak in the center of the fault plane reflections where present and/or by following the offsets in strata that separate the imbricate thrust sheets. The majority of the imbricate thrust faults could be traced from

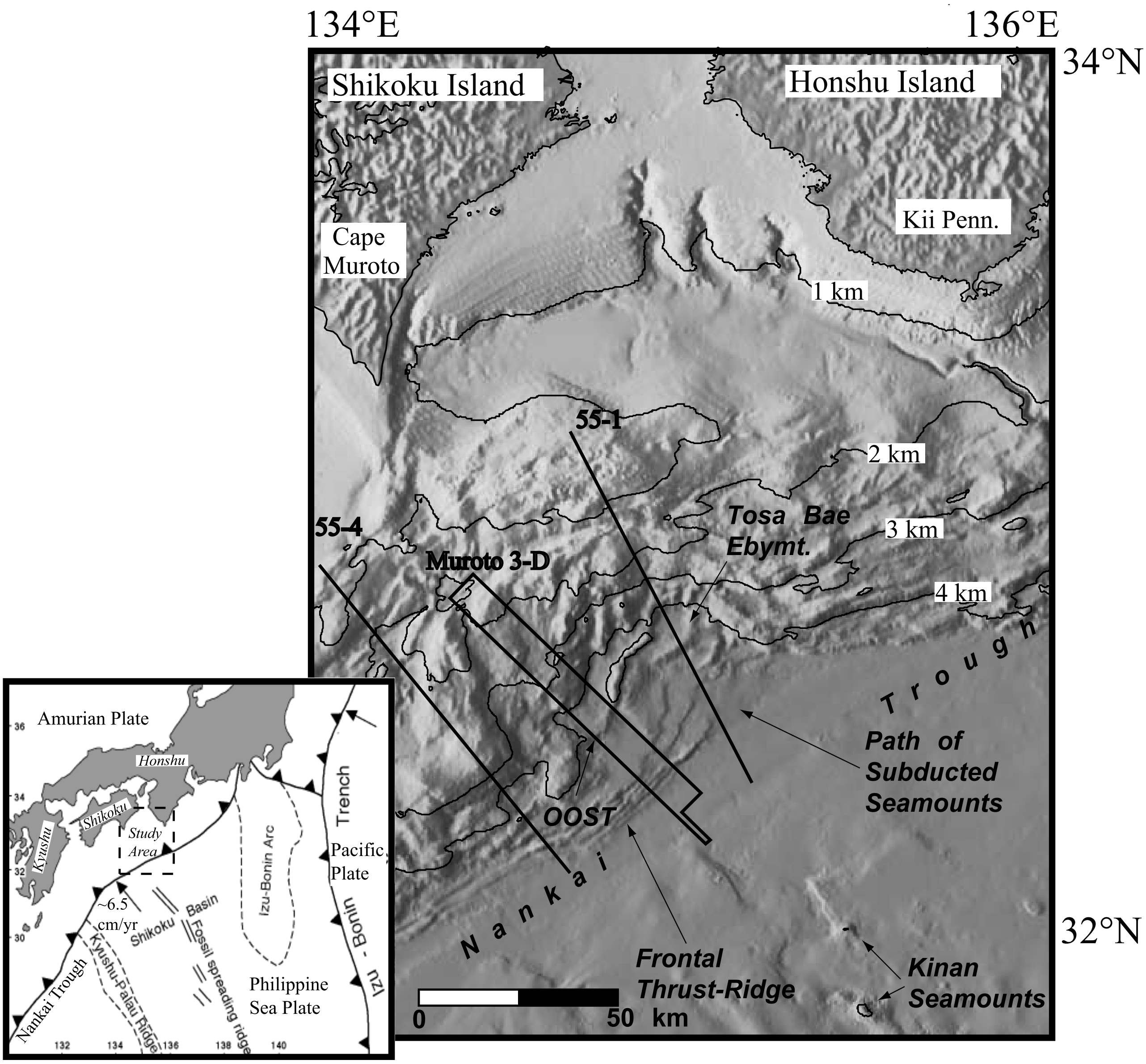

Figure 1. Study area for the Nankai 3-D seismic experiment. Inset shows location relative to Japan with box delineating study area. The Tosa Bae embayment is shown most clearly by the 4 km bathymetric contour.

near the décollement to close to the seafloor, however our confidence in our interpretation, while generally quite high due to the high quality of the data, decreases somewhat landward.

3. Results

[10] The outer accretionary prism off Muroto is highly deformed by a series of thrust faults that splay off a subhorizontal décollement generating a zone of imbricate thrust slices (the imbricate thrust zone) and incipient thrust slices (the protothrust zone) (Figures 2, 4, and 5). We examine these thrust slices and the faults in detail using the Muroto 3-D volume to reveal the architecture of the outer accretionary prism. Our observations are divided into three categories: seafloor observations, prism architecture and fault geometries, and correlation of seafloor relief with major thrust slices.

3.1. Seafloor Observations

[11] One of the useful by-products of 3-D seismic reflection data is a well-imaged seafloor, which at a resolution of 25×50 m is actually improved over the publicly available seafloor bathymetry for the Nankai Trough off Cape Muroto, Shikoku Island. Figure 2 shows a shaded relief map of the seafloor from the first out-of-sequence thrust to the deformation front.

[12] The seafloor image (Figure 2) shows the minimal seafloor expression of the protothrust zone, a series of clearly defined seafloor ridges that are surprisingly variable across the width of the survey within the imbricate thrust zone, and two prominent seafloor ridges related to the out-

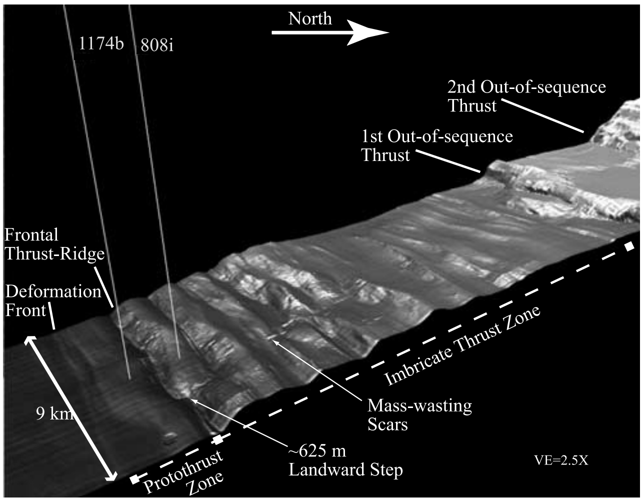

Figure 2. Westward looking 3-D perspective view of the seafloor within the 3-D volume. The seafloor image was interpreted from the seismic data and has a 25 m inline by 50 m crossline resolution. The major structural features for the outer portion of the prism are shown along with the ODP boreholes 808 and 1174. This paper concentrates on the protothrust and imbricate thrust zones.

of-sequence thrust just landward of the imbricate thrust zone and at the base of a steeply sloping portion of the prism known as the large-thrust slice zone. Within the imbricate thrust zone, the majority of the seafloor ridges do not cut across the entire width of the volume. Several of the ridges appear to change orientation along strike as well as exhibiting differing amounts of relief. The location of the greatest change appears to be approximately 2.25 km southwest of the northeastern edge of the volume where the deformation front and the seafloor ridge related to the frontal thrust step landward and the majority of the seafloor ridges either terminate or change orientation. While a series of mass-wasting scars visible on the seafloor do seem to line up with the landward step in the frontal thrust, there is no singular dip direction oriented, throughgoing feature that would suggest a fault cutting perpendicular to the margin. More regionally, the clear landward step in the frontal thrust and the largely landward steps observed 2.25 km from the northeastern edge of the 3-D volume appear to be part of a series of landward steps in the seafloor ridges progressing from southwest to northeast into the Tosa Bae embayment (Figure 1).

3.2. Prism Architecture and Fault Geometries

[13] Across the 9 km width of the 3-D volume, we observe a series of thrust faults that strike generally orthogonal to subduction direction (Figure 4); however, the seafloor relief, fault complexities, and patterns of faulting within the imbricate thrust zone vary significantly along strike. These variations in the subsurface clearly explain, among other things, the landward step in seafloor ridge generated by the frontal thrust.

[14] From southwest to northeast, within the 3-D volume, we observe along-strike changes in the protothrust zone and at the frontal thrust. The protothrust zone consists of two prominent faults. The first stretches from southwest to northeast across 6.5 km of the imaged 9 km of the prism before terminating and being replaced by a second fault plane that lies ~625 m closer to land (Figure 4). The frontal thrust similarly stretches across the imaged portion of the prism as a single gently undulating fault plane for 6.5 km before stepping landward en echelon to an entirely different frontal thrust. A ~625 m landward step is observed, therefore, both at the deformation front seaward of the protothrust one and in the frontal thrust and overlying seafloor ridge that divides the protothrust zone from the imbricate thrust zone (Figure 2 and 4a). As with the examination of the seafloor in this area (Figure 2), the ~625 m landward step in the protothrust zone and the frontal thrust is not caused by any kind of observable deformation perpendicular to the margin. The lack of down-dip deformation is demonstrated by crossline 800, which shows the 3-D volume parallel to the deformation front, and clearly images the two frontal thrusts overlapping along strike; however, it does not show them being interconnected by any seismically imageable faulting (Figure 5). In other words, there is no transfer zone imaged within the accreting sediments, although these faults are linked by the décollement.

[15] Both these frontal thrusts, the two protothrusts, and nearly all the remaining imaged faults of the imbricate thrust zone show complexities such as fault splays, backthrusts, or even pairs of piggyback faults jointly involved in generating a particular thrust ridge (Figure 4). To examine the observations in detail, we will look at the interpreted faults in

PROCESSING FLOW FOR NANKAI 3-D DATA

SEG-D FIELD DATA
↓
RESAMPLE to 4 ms
↓
SEG-Y DATA
↓
FILTER 5-8-65-80 Hz
↓
TRACE/SHOT KILLS
↓
SORT-Common Offset Xline Gathers
↓
Trace Interpolation in Xline Direction
↓
SORT-3-D Bins
↓
NMO
↓
Outside Stretch Mute
↓
Inside Water bottom Multiple Mute
↓
Surgical Far Offset Crustal Mute
↓
3-D STACK
↓
Post-stack Decon
↓
Post-stack Time Migration
↓
Conversion to Depth

Figure 3. Processing flow for the depth converted, crossline interpolated, poststack time migrated 3-D volume.

a.

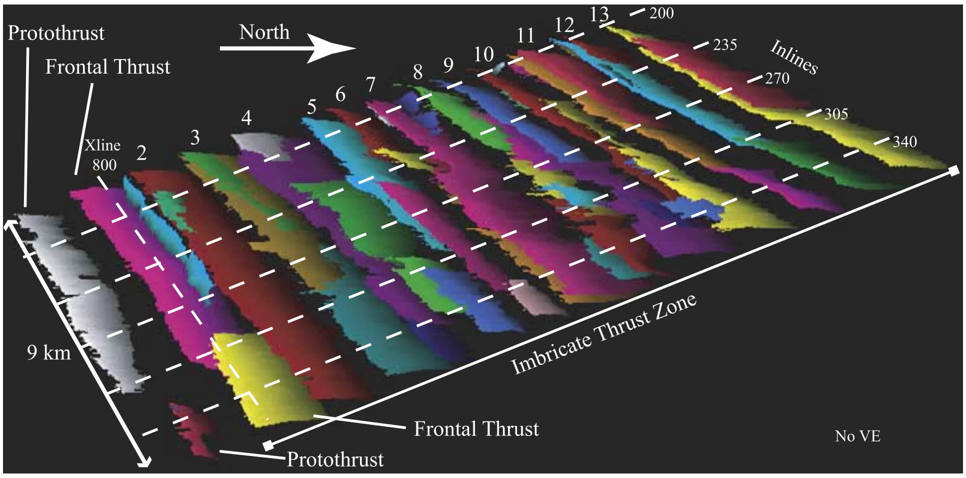

b.

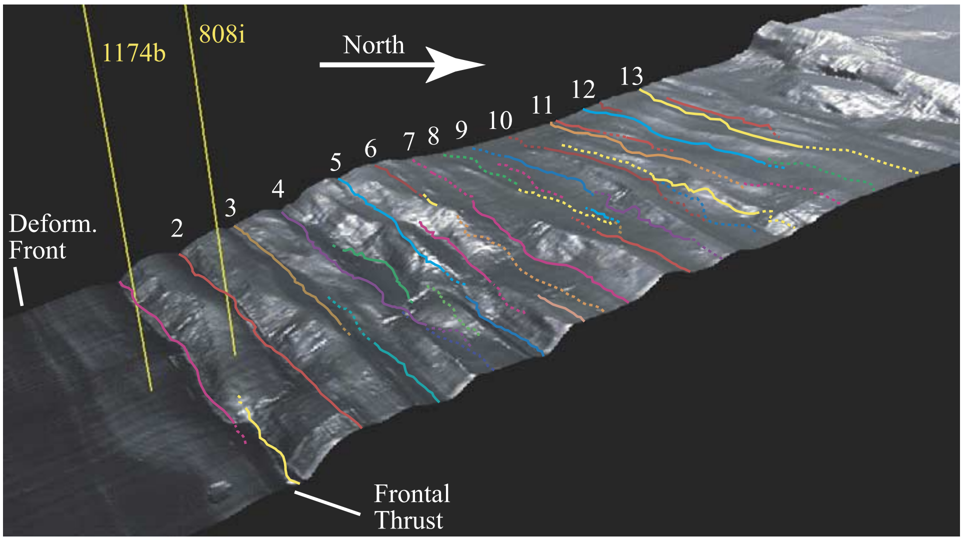

Figure 4. (a) The 3-D perspective view from the southeast of all the interpreted faults for the outer portion of the Nankai 3-D volume. Each colored surface is a different fault plane (note many colors repeat) as viewed from the same perspective as the seafloor in Figure 3 but with no vertical exaggeration. The locations of the five inlines and one crossline shown in two dimensions in Figures 5 and 6 are displayed as dashed lines. Thrust slices along the southwestern edge of the 3-D volume are labeled for reference (see text for explanation). (b) Same seafloor relief as in Figure 3 with the primary thrust faults extended to the seafloor. Colors match Figure 4a, and dashed lines represent more deeply buried faults.

three dimensions (Figure 4a) and on five, representative dip direction transects (inlines 200, 235, 270, 305, and 340, Figures 6a–6e). Figure 4a shows the locations of these lines and the numbering of the thrusts from the deformation front landward; the color of the thrusts match on Figures 4 and 6 for ease of correlation.

[16] With the exception of the second and the thirteenth thrusts which cut completely across the Muroto 3-D volume, the majority of the imaged thrusts do not cut across the volume but rather consist of smaller overlapping en echelon faults of varying lengths (Figures 4 and 6). The regional en echelon pattern of the third, fifth–seventh, tenth, and twelfth thrusts are landward stepping to the northeast while the eighth series of thrusts step seaward and the fourth series of thrusts step first seaward and then landward. Detailed examination of this en echelon architecture reveals that when one fault is replaced by another along strike the two faults will overlap for a few inlines (usually 100–250 m) before terminating in opposite directions. For example, the 3rd thrust on the southwestern side of the 3-D volume (light brown in Figure 4a), which cuts nearly to the seafloor on inlines 200–270 (Figures 6a–6c), diminishes greatly in its updip extent on inline 305 (Figure 6d), while the third thrust on the northeastern side of the 3-D volume (blue-green on Figure 4a), which is the dominant thrust plane on inlines 305 and 340, can be seen to be terminating on inline 270 (Figures 6c–6e). The dominance of this en echelon style deformation persists throughout the imbricate thrust zone (Figure 4a).

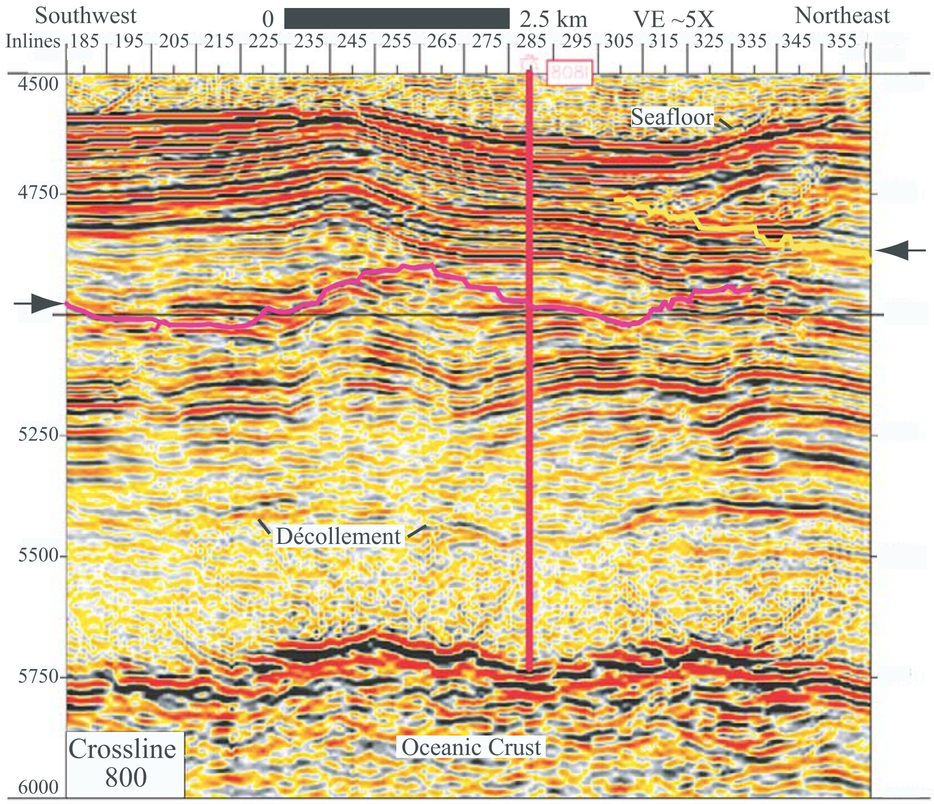

Figure 5. Depth section for crossline 800 showing the two different frontal thrust fault planes. Note that there is no interconnection between the fault planes nor any evidence for any northwest-southeast oriented faulting. Vertical exaggeration is ~5X.

[17] Additional complexities along strike include faults that transition into pairs of thrusts, as observed in the fourth, seventh, and twelfth series of thrusts, and faults that are replaced along strike with little or no overlap as in the ninth and eleventh thrusts. When faults transition into pair of thrusts there appears to be no evidence of the thrusts interconnecting, except via the décollement, but rather they frequently overlap for a few hundred meters along strike keeping with the en echelon pattern. In places there are examples of piggyback thrusts which persist for greater distances such as the second thrust on inline 340 (Figure 6e) in the northeast which by piggybacking on the frontal thrust appears to dome the overlying seafloor (Figure 4b). Last, all thrusts within the imbricate thrust zone parallel the deformation front for the width of the 3-D volume with the exception of the northeastern ends of the three landward-most thrust slices that exhibit a slight landward curvature (Figures 4a and 4b).

3.3. Correlation of Seafloor Relief With Major Thrust Slices

[18] Since seafloor relief is often used as a proxy for fault activity it is important to evaluate the association of seafloor features with the primary subsurface fault systems. In general, the series of thrusts generate seafloor relief throughout the imbricate thrust zone with the exception of a small region, three to five thrusts wide on the southwestern side of the volume where the thrusts are buried by sediment (thrusts 7–10 on inline 200 and thrusts 6–8 on inline 235, Figures 6a and 6b). The outer five to six thrust ridges display consistently greater seafloor relief suggesting a greater level of recent throw on the outer few younger thrusts, however the majority of the more landward and older thrusts of the imbricate thrust zone remain active up to the first out-of-sequence thrust (Figures 4 and 6). Many of the locations of greatest local seafloor relief are on morphologic ridges generated by pairs of piggyback thrust faults such as CDP 950 on Figures 6b and 6c, CDP 1050 on Figures 6d and 6e and the frontal thrust on Figure 6e.

[19] Although the underlying imbricate thrusts clearly generate seafloor relief, the pattern of seafloor ridges along-strike does not reflect underlying en echelon thrust architecture (Figure 4b). Figure 4b shows the planes of the primary thrust faults extended to the seafloor (colors match Figure 4a) where the dashed lines are those fault planes that are deeply buried (i.e., less active or terminating along strike) and the solid lines are those fault planes that are prominent although do not necessarily intersect the seafloor. Note the clear pattern of en echelon faults is revealed when only the primary thrust planes are examined (Figure 4b). The generally sinuous nature of the seafloor morphology does not match the primary thrust faults and the exact location of the seafloor intersection of the primary thrust planes is sometimes not at the base of a morphologic ridge. For example, the 5th thrust if interpreted just based on the overlying thrust ridge it would appear to snake across the

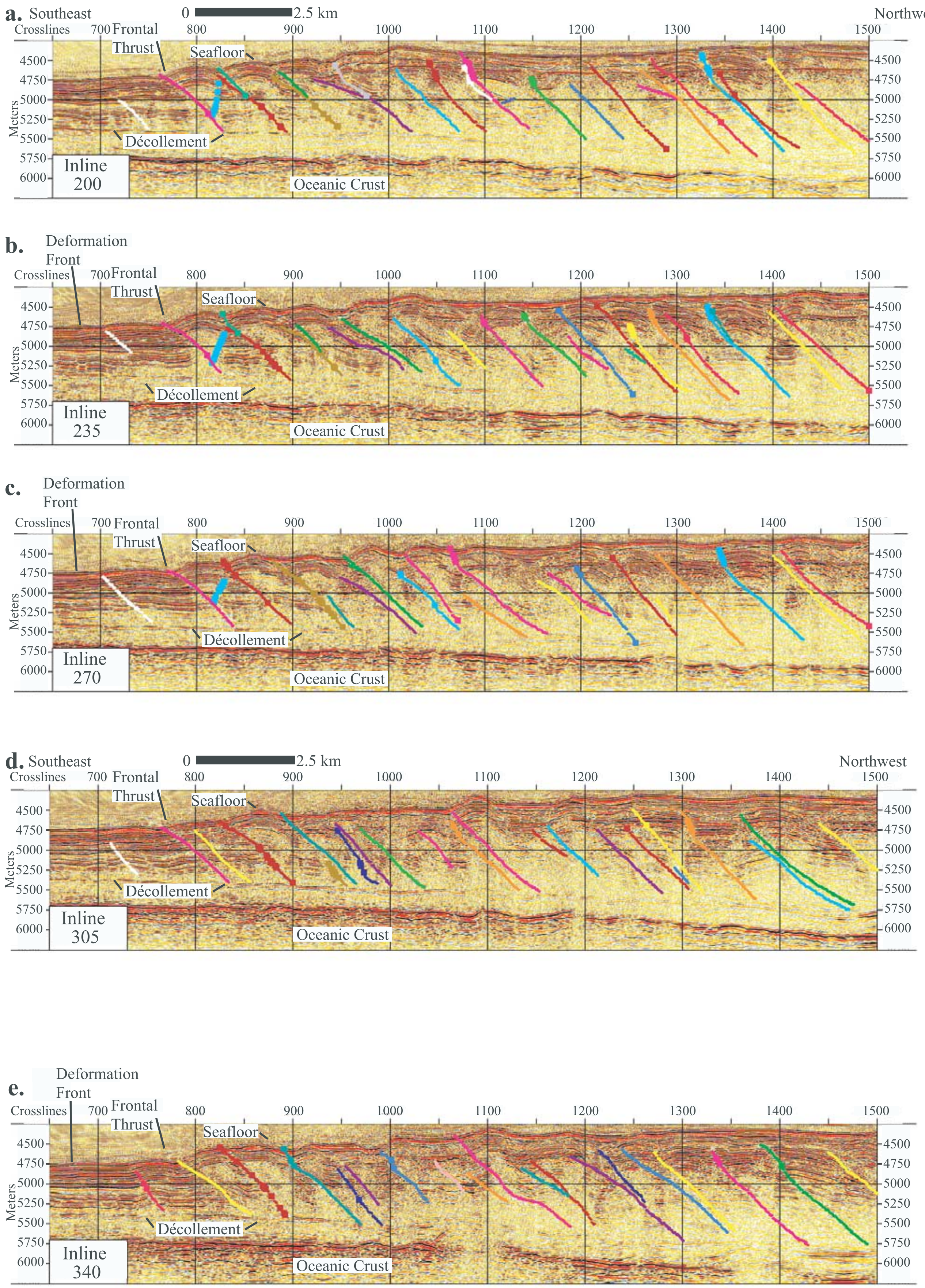
a. Southeast
0
2.5 km
Northwest
Crosslines
Frontal Thrust
Seafloor
Décollement
Inline 200
Oceanic Crust
Meters
b. Deformation Front
Inline 235
c. Deformation Front
Inline 270
d. Southeast
Northwest
Inline 305
e. Deformation Front
Inline 340

Figure 6.

study area curving first landward and then back seaward before terminating ~2 km from the northeastern edge of the volume. When in reality, the projected surface trace of the fifth thrust (blue on Figure 4b) starts at the base of the fifth ridge on the southwestern edge of the volume but unlike the overlying ridge continues nearly straight northeast cutting across the crest of the fourth ridge and then dies out ~3 km from the northeastern edge of the volume. In other words, the fifth morphologic ridge in the southwestern and central portions of the survey is actually generated by 2 different thrusts in an en echelon pattern and there is no single fault that snakes across the survey at the base of the ridge as might be assumed from examining the bathymetry alone.

4. Discussion

[20] Within the Muroto 3-D volume, individual fault complexities as well as the patterns of the major fault planes vary significantly along strike with a few basic observations: (1) all the fault planes are generally parallel to the deformation front, (2) within the imbricate thrust zone the thrusts have similar dips and splay off the décollement at similar angles, (3) the fault planes rarely curve along strike but rather as the scallop-shaped embayment is approached faults frequently overlap landward in an en echelon pattern, (4) none of the changes in faulting along strike are accommodated by interconnected lateral fault ramps, (5) numerous faults exhibit high-order complexities such as backthrusts and fault splays that vary significantly along strike, (6) the en echelon fault pattern is not clearly reflected in the seafloor morphology, with the exception of the seafloor ridge generated by the frontal thrust, and (7) the details of the seafloor morphology are more closely tied to the high-order complexities of the faulting rather than the patterns of the main fault planes that sole into the décollement (Figure 4b). Among these observations, the changes in numbers of thrust slices, the presence of backthrusts or splay faults, and even the occasional pairs of piggyback faults generating a single thrust slice are likely examples of natural variability in prism architecture (Figures 4 and 6a–6c). It is possible that the en echelon pattern of faulting is common in accretionary prisms but has previously not been imaged due to the lack 3-D seismic data. However, the consistent landward stepping observed within the Muroto 3-D volume in the direction of the Tosa Bae embayment suggests some along-strike changes in wedge geometry related to prism reconstruction after seamount subduction.

4.1. Causes of En Echelon Fault Architecture

[21] Overprinting the natural along-strike variability within the prism are significant changes in prism architecture that are likely related to larger tectonic events. For the Muroto 3-D volume, there is a clear change that occurs between inlines 310 and 320 where the deformation front and frontal thrust step landward ~625 m and major prism architecture reorganization occurs (Figures 3 and 4). The along-strike variability in the architecture of the thrust slices increases greatly surrounding this landward step region apparently in order to transition from the deformation regime that is dominant in the southwestern portion of the 3-D volume to the one present in the northeastern portion of the volume. The mechanism of transition between differing prism architectures seems to be one of overlapping, en echelon, fault planes that do not interconnect as seen by examining the faults in 3-D (Figure 4) and on crosslines (e.g., Figure 5). There must be some accommodation of strain in between the overlapping segments en echelon thrusts but strain within these "transfer zones" is either discrete but at a scale below our resolution, or diffuse (within the sediments).

[22] The one locale within the 3-D volume that does exhibit curved thrusts is the northeastern end of the 3 landwardmost structures (Figure 4). These faults lie beneath a smooth domed seafloor and may therefore be less or inactive. The curvature of these faults may then reflect the increasing importance of volume-strain processes within the more landward portions of the prism where differential stress along-strike shear the sediments volumetrically and thus these older faults are acting like marker beds to show the differential strain along strike.

[23] En echelon fault patterns are common in thrust belts and continental margins undergoing transpression, but have not been previously observed at the toe of accretionary prisms. There is, however, no reported evidence for transpressive stresses within the Nankai accretionary prism; instead the accretionary prism is formed with a nearly trench-normal compression as shown by a borehole breakout in Hole 808I during ODP Leg 196 [*Mikada et al.*, 2002] and the available earthquake focal mechanisms and moment tensors [e.g., *Ando*, 1975].

[24] The lack of clearly observed en echelon faulting prior to this study may simply reflect the paucity of 3-D data in accretionary prism environments. We suggest that en echelon fault architecture is likely common in accretionary prisms that undergo significant geometric curvatures along strike, such as those created by seamount subduction, and possibly in accretionary prisms with other significant along-strike changes such as sediment type or volume, and subduction of basement topography.

4.2. Geometry: Implications for Basal Shear Strength and Prism Rebuilding

[25] In order to further examine the cause of the systematic en echelon fault pattern, we examine the 3-D geometry of the décollement to look for any along-strike changes that might cause prism reorganization. Additionally, we have calculated a set of accretionary wedge geometry parameters southwest and northeast of this prominent change in architecture in order to look for relevant changes in the prism characteristics.

[26] The obvious explanation for the dramatic along-strike architecture change is some sort of along-strike or down-dip change in the geometry of the décollement possibly generated by underlying basement structure. However, as Figure 7a shows there are no significant structural

Figure 6. Five 2-D depth sections from within the outer portion of the 3-D volume. Locations are shown in Figure 4a. Depth sections of the imbricate thrust zone on inlines 200, 235, 270, 305, and 340 are shown at identical scales for comparison and with a vertical exaggeration of ~2.3X.

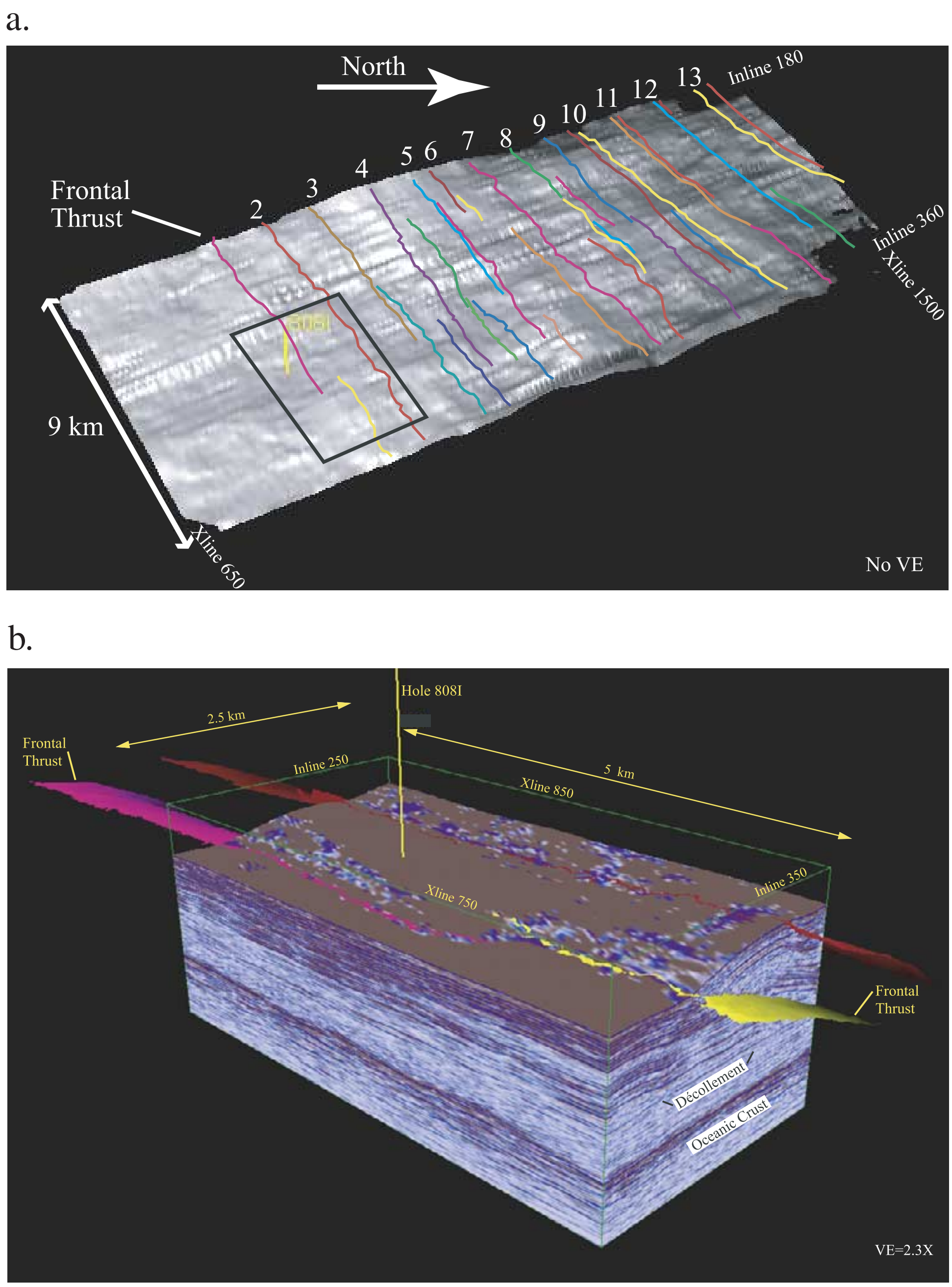

Figure 7. (a) The 3-D perspective of décollement with the approximate locations that each of the major thrust faults sole into the décollement. There are no apparent structural features that could explain the en echelon architecture of the overlying imbricate thrusts. Black polygon shows area of Figure 7b. (b). The 3-D perspective view of décollement between inlines 310 and 320 showing the lack of along-strike structural change.

changes in the décollement surface that adequately explain en echelon architecture within the imbricate thrust zone. Furthermore, a blowup between inlines 310 and 320 (the area of the prism reorganization) demonstrates the décollement remains flat along-strike beneath the en echelon frontal thrusts (Figure 7b).

[27] The accretionary wedge parameters that may change along strike in addition to the any changes in the geometry of the décollement include the upper and lower taper angles which can be used to calculate basal shear stress, the ratio of subducting versus accreting sediment, the total volume of accreted and subducted sediments, and the thrust spacing which are shown in Table 1. For continuity, we will examine the wedge geometry parameters on the same five representative inline profiles within the Muroto 3-D volume shown in Figure 6, and for comparison, we will look at these same parameters on two nearby 2-D industry lines, 55-1 and 55-4 (see Figure 1 for location). Convergence direction and the rate of the subducting plate are assumed constant across this portion of the prism.

Table 1. Accretionary Wedge Parameters of Seven Profiles[a]

Transect	α, deg	β, deg	μb, φ = 24.4°	μb, φ = 20°	Subducted Sediments, m	Accreting Sediments, m	Volume ITZ, km^2	Thrust Spacing, km
55-4	1.7	0.4	0.081	0.067	250	690	16.7	1.5
200	1.3	1.7	0.095	0.076	340	670	20.7	1.4
235	1.4	1.7	0.103	0.082	310	660	19.8	1.4
270	1.5	1.6	0.101	0.081	280	700	18.7	1.5
305	1.5	1.6	0.101	0.081	290	690	20.4	1.6
340	1.9	1.6	0.119	0.096	330	640	16.2	1.4
55-1	0.9	1	0.063	0.050	360	810	26.7	1.7

[a]Profile 55-4 lies southwest of, 200–340 are inlines of, and 55-1 lies northeast of the Muroto 3-D volume.

[28] The outermost portion of the Nankai Trough accretionary prism imaged by the 3-D survey and neighboring 2-D industry profiles is fairly uniform in terms of taper angles alpha (α) and beta (β) (Table 1) [*Dahlen et al.*, 1984; *Davis et al.*, 1983]. Using these taper angle values we calculate approximate basal shear stresses according to the method presented by *Gulick et al.* [1998]. Two angles of internal friction (φ) were tested: 24.4° determined by *Feeser et al.* [1993] from ODP Hole 808c samples and 20° calculated by *Karig and Lundberg* [1990] from deformation bands in cores obtained on DSDP Legs 31 and 87A assuming Coulomb mechanics. The method presented by *Gulick et al.* [1998] assumes that the pore pressure within the wedge and at the base to be equal, and calculates effective friction coefficients which are a combination of intrinsic strength and elevated pore pressure.

[29] As Table 1 shows, the basal shear stress values are very low on all five Muroto 3-D transects. The upper taper angle (α) for line 55-4 is similar to the profiles on the Muroto transect at ~2° while (α) for line 55-1 within the portion of the prism that has been directly rebuilt after the latest phase of Kinan seamount subduction is the lowest observed at only ~1° (Table 1). The basal taper angles (β) for 55-4 and 55-1 are both less than the profiles in the Muroto 3-D transect with values of ~1° (Table 1). The fact that all 7 transects have very low basal shear stress shows that the change in architecture 6.5 km across the 3-D volume is not related to basal friction.

[30] The ratios of subducting versus accreting sediments are also similar on all 7 transects with an average of ~2/3 of incoming Shikoku basin sediments being currently accreting to the margin while ~1/3 of the incoming sediments being subducted at the toe of the prism (Table 1). However, our calculations of the areas of sediments within the imbricate thrust zone (volume ITZ in Table 1), which approximately represent the size of the modern prism (all accretion seaward of the first out-of-sequence thrusting) are different seaward of the Tosa Bae embayment (line 55-1) then elsewhere. Instead of these values being correlative along this portion of the margin, the amount of accreted sediment on line 55-1 is significantly larger than the volume of the imbricate thrust zone within the Muroto 3-D volume or on line 55-4. Furthermore, the spacing of thrust slices on the 2-D transect within the Tosa Bae embayment is larger (1.7 km) than the spacing of the thrusts within the Muroto 3-D volume and to the southwest of it (avg. 1.46 km) (thrust spacing in Table 1). These observations combined with the slightly shallower taper of the prism (Table 1) suggest that accelerated rebuilding occurred within the Tosa Bae embayment following the latest seamount subduction. Our results are consistent with the work of *Saffer and Bekins* [2002], which showed faster outbuilding leads to larger basal pore pressures and a shallower taper angle.

[31] Our observations that the major imbricate thrust faults all remain approximately perpendicular to the convergence direction despite the perturbation to margin geometry due to seamount subduction, suggest that the imbricate thrusts are dominated by the regional convergence-generated compression not local stress variations. When a large perturbation to the system occurs such as subduction of a seamount, the major fault planes do not curve to accommodate the produced curvature of the margin, but instead remain perpendicular to convergence direction, due to a kinematic connection with the regional décollement, and propagate en echelon laterally to remove the perturbation.

[32] On the basis of the images from the Muroto 3-D volume we propose a hypothesis for the process of prism reconstruction that involves not only rapid accretion in the damaged area, but propagation of thrust faults from neighboring undamaged portions of the prism into the damaged zone (Figure 8). Because of the geometric perturbation caused by the seamount subduction, these fault zones step landward en echelon into the embayment or damaged zone and spread apart to allow for more rapid prism rebuilding. This process continues until the deformation front is once again continuous and perpendicular to convergence. For the Muroto3-D volume, the obvious change in prism architecture observed in the 2.25 km of the volume closest to the embayment appears to be the first of several major en echelon landward steps into the embayment. The envisioned process is hinted at in Figure 1, where the outer thrust ridges northeast of the 3-D volume step en echelon landward and widen to the northeast into the embayment. Note that our hypothesis would predict that as the prism rebuilds itself there is less of a curvature to the margin and thus less extreme en echelon style faulting is required. Younger, more seaward thrusts would either step landward more gently as hinted at in the seafloor ridges in Figure 1 or would consist of longer segments thus stepping landward less frequently (as shown in Figure 8).

4.3. Structures and Seafloor Relief

[33] Our interpretation of the observed disconnect between seafloor morphology and subsurface structural architecture is that the details of the seafloor morphology are a combination of two effects. (1) The seafloor ridges

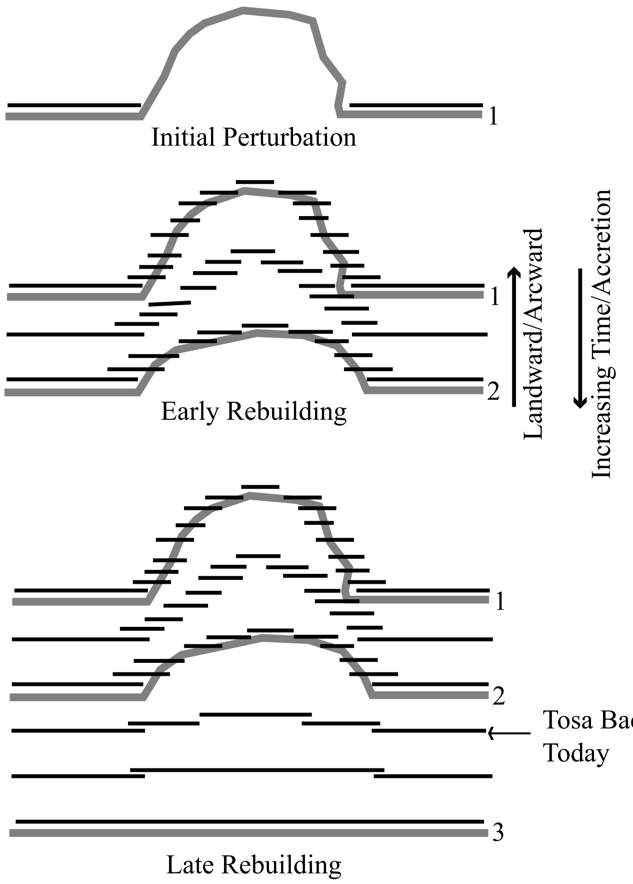

Figure 8. Proposed hypothesis for the mechanism by which accretionary prisms "heal" damage generated by seamount subduction. Bold grey lines are successively younger deformation fronts (numbered 1–3), while thin black lines are thrust faults. Note that during rebuilding, the spacing between the series of en echelon thrusts is wider in the damaged zone than the surrounding prism (faster accretion and lower taper angle). As the prism is rebuilt, the thrust spacing narrows (thus accretion slows down and prism taper increases) until reaching the average thrust spacing that matches the neighboring undamaged prism. We mark the approximate condition that rebuilding seaward of the Tosa Bae embayment has reached today.

effectively generate smoothed reflections of the active subsurface faulting. (2) The details of the seafloor relief are modified substantially by movements on higher-order shallow features such as splay thrusts and back thrusts, and by interactions between faults such as piggyback thrusts. The smoothing effect of the seafloor, which would be enhanced on margins with rapid sediment accumulation, is why the en echelon architecture of the primary fault planes is not reflected in the seafloor morphology. The second-order faulting such as near-surface splay faults have not been fully interpreted within this data set but generally speaking there is a greater complexity of faulting visible in the upper 250 m and it is these smaller faults that often connect the seafloor ridges with the primary fault planes. The specific orientation of these higher-order faults is frequently quite different than the primary décollement related faults so that the seafloor morphology may not accurately reflect the primary subsurface fault geometries.

5. Conclusions

[34] Using the Muroto 3-D seismic reflection volume for a detailed examination of the thrust faults in the imbricate thrust zone and protothrust zone shows that (1) all primary thrust fault planes remain parallel to the deformation front and have similar dips, (2) numerous faults exhibit high-order complexities such as backthrusts and fault splays that vary significantly along strike, (3) a clear change in structural architecture is observed 2.25 km from the northeastern edge of the 3-D volume that appears to be the first of a series of northeastward oriented landward stepping zones of deformation that propagate into the Tosa Bae embayment in order to facilitate prism reconstruction, (4) the Tosa Bae embayment, which was caused by the subduction of the Kinan seamounts, is locally a geometric anomaly that is accommodated structurally by fault planes stepping landward in an en echelon pattern rather than curving along strike, (5) the deformation front-parallel en echelon fault pattern is not clearly reflected in the seafloor morphology suggesting caution should be used in interpreting regional fault patterns and especially fault continuity based on seafloor morphology alone, and (6) the details of the seafloor morphology are more closely tied to the high-order complexities of the faulting rather than the patterns of the main fault planes that sole into the décollement. The results of this study imply that accretionary prisms have a built-in mechanism of reattaining equilibrium following seamount subduction by lateral en echelon fault propagation into damaged zones that facilitate an increase accretion rate until a laterally continuous deformation front is reestablished.

[35] **Acknowledgments.** We wish to thank the Captain and crew of the R/V *Maurice Ewing* for their exemplary aid throughout the 63 day data seismic acquisition cruise. We recognize the navigation and processing assistance of Mark Wiederspahn, Zhao Zhiyong, and Steffen Saustrup. This manuscript benefited from excellent reviews by Demian Saffer, Dan Lizarralde, and Geoff Abers. Research supported by National Science Foundation grants NSF-OCE-9730637 to the University of Texas at Austin and NSF-OCE-9802295 to the University of Hawaii. Additional support provided by the Science and Technology Agency of Japan through the Geological Survey of Japan and the University of Tokyo. UTIG contribution 1660 and SOEST contribution 6298.

References

Ando, M. (1975), Source mechanisms and tectonic significance of historical earthquakes along the Nankai Trough, *Japan, Tectonophysics*, *27*, 119–140.

Aoki, Y., T. Tamano, and S. Kato (1982), Detailed structure of the Nankai Trough from migrated seismic sections, in *Studies in Continental Margin Geology*, edited by J. S. Watkins and C. L. Drake, *AAPG Mem.*, *34*, 309–322.

Aoki, Y., H. Kinoshita, and H. Kagami (1986), Evidence of a low-velocity layer beneath the accretionary prism of the Nankai Trough: Inference from a synthetic sonic log, *Initial Rep. Deep Sea Drill. Proj.*, *87*, 727–735.

Ashi, J., H. Tokuyama, F. Yamamoto, T. Uyeki, H. Tukioka, and A. Taira (1989), Detailed surface features of the Nankai accretionary prism obtained by IZANAGI oceanfloor imaging sonar system, *Program Abstr. Seismol. Soc. Jpn.*, *2*, 305.

Bangs, N. L., et al. (1999), U.S.-Japan Collaborative 3-D seismic investigation of the Nankai Trough plate-boundary interface and shallowmost seismogenic zone, *Eos Trans. AGU*, *80*(46), Fall Meet. Suppl., F569.

Byrne, T., W. Bruckmann, W. Owens, S. Lallemant, and A. Maltman (1993), Structural synthesis: Correlation of structural fabrics, velocity anisotropy, and magnetic susceptibility data, *Proc. Ocean Drill. Program Sci. Results*, *131*, 365–378.

Dahlen, F. A., J. Suppe, and D. Davis (1984), Mechanics of fold-and-thrust belts and accretionary wedges: Cohesive Coulomb theory, *J. Geophys. Res.*, *89*, 10,087–10,101.

Davis, D., J. Suppe, and F. A. Dahlen (1983), Mechanics of fold-and-thrust belts and accretionary wedges, *J. Geophys. Res.*, *88*, 1153–1172.

Feeser, V., K. Moran, and W. Brückmann (1993), Stress-regime-controlled yield and strength behavior of sediment from the frontal part of the Nankai accretionary prism, *Proc. Ocean Drill. Program Sci. Results*, *131*, 261–274.

Gulick, S. P. S., A. S. Meltzer, and S. H. Clarke Jr. (1998), Seismic structure of the southern Cascadia subduction zone and accretionary prism north of the Mendocino Triple Junction, *J. Geophys. Res.*, *103*, 27,207–27,222.

Kaiko I Research Group (1986), *Topography and Structure of Trenches Around Japan—Data Atlas of Franco-Japanese Kaiko Project, Phase I*, Univ. of Tokyo Press, Tokyo.

Karig, D. E., and N. Lundberg (1990), Deformation bands from the toe of the Nankai accretionary prism, *J. Geophys. Res.*, *95*, 9099–9109.

Kodaira, S., N. Takahashi, J. Park, K. Mochizuki, M. Shinohara, and S. Kimura (2000), Western Nankai Trough seismogenic zone: Results from a wide-angle ocean bottom seismic survey, *J. Geophys. Res.*, *105*, 5887–5905.

Kuramoto, S., et al. (2001), Surface observations of subduction related mud volcanoes and large thrust sheets in the Nankai subduction margin: Report on YK00-10 and YK01-04 cruises, *JAMSTEC J. Deep Sea Res.*, *19*, 131–139.

Leggett, J., Y. Aoki, and T. Takefumi (1985), Transition from frontal accretion to underplating in a part of the Nankai Trough Accretionary Complex off Shikoku (SW Japan) and extensional features on the lower trench slope, *Mar. Pet. Geol.*, *2*, 131–141.

LePichon, X., et al. (1987a), Nankai Trough and fossil Shikoku Ridge results of Box 6 Kaiko survey, *Earth Planet Sci. Lett.*, *83*, 186–198.

LePichon, X., et al. (1987b), Nankai Trough and Zenisu Ridge: A deep-sea submersible survey, *Earth Planet Sci. Lett.*, *83*, 285–299.

Maltman, A. J., T. Byrne, D. E. Karig, S. Lallemant, R. Knipe, and D. Prior (1993), Deformation structures at Site 808, Nankai accretionary prism, Japan, *Proc. Ocean Drill. Program Sci. Results*, *131*, 123–133.

Mikada, H., et al. (2002), *Proceedings of the Ocean Drilling Program, Initial Reports*[CD-ROM], vol. 196, Ocean Drill. Program, College Station, Tex.

Mikada, H., et al. (2003), Hydrologeological and geothermal studies around Nankai Trough (KR02–10 Nankai Trough cruise report), *JAMSTEC J. Deep Sea Res.*, *22*, 125–171.

Miyazaki, S., and K. Heki (2001), Crustal velocity field of southwest Japan: Subduction and arc-arc collision, *J. Geophys. Res.*, *106*, 4305–4326.

Moore, G. F., and T. H. Shipley (1993), Character of the decollement in the Leg 131 area, Nankai Trough, *Proc. Ocean Drill. Program Sci. Results*, *131*, 73–82.

Moore, G. F., T. H. Shipley, P. L. Stoffa, D. E. Karig, A. Taira, S. Kuramoto, H. Tokuyama, and K. Suyehiro (1990), Structure of the Nankai Trough accretionary zone from multichannel seismic reflection data, *J. Geophys. Res.*, *95*, 8753–8765.

Moore, G. F., D. E. Karig, T. H. Shipley, A. Taira, P. L. Stoffa, and W. T. Wood (1991), Structural framework of the ODP Leg 131 area, Nankai Trough, *Proc. Ocean Drill. Program Initial Rep.*, *131*, 15–20.

Moore, G. F., et al. (2001a), Data report: Structural setting of the Leg, 190 Muroto transect, data report, *Proc. Ocean Drill. Program Initial Rep.* [CD-ROM], *131*, 1–14.

Moore, G. F., et al. (2001b), *Proceedings of the Ocean Drilling Program, Initial Reports*[CD-ROM], vol. 190, Ocean Drill. Program, College Station Tex.

Moore, G. F., et al. (2001c), New insights into deformation and fluid flow processes in the Nankai Trough accretionary prism: Results of Ocean Drilling Program Leg 190, *Geochem. Geophys.*, 2, paper number 2001GC000166.

Morgan, J. K., and D. E. Karig (1995), Kinematics and a balanced and restored cross-section across the toe of the eastern Nankai accretionary prism, *J. Struct. Geol.*, *17*, 31–45.

Nasu, N., et al. (1982), Multichannel seismic reflection data across Nankai Trough, report, Ocean Res. Inst., Univ. of Tokyo, Tokyo.

Ohmori, K., A. Taira, H. Tokuyama, A. Sagaguchi, M. Okamura, and A. Aihara (1997), Paleothermal structure of the Shimanto accretionary prism, Shikoku, Japan: Role of an out-of-sequence thrust, *Geology*, *25*, 327–330.

Okino, K., Y. Shimakawa, and S. Nagaoka (1994), Evolution of the Shikoku basin, *J. Geomagn. Geoelectr.*, *46*, 463–479.

Park, J.-O., T. Tsuru, Y. Kaneda, Y. Kono, S. Kodaira, N. Takahashi, and H. Kinoshita (1999), A subducting seamount beneath the Nankai accretionary prism off Shikoku, southwestern Japan, *Geophys. Res. Lett.*, *26*, 931–934.

Park, J.-O., T. Tsuru, S. Kodaira, A. Nakanisi, S. Miura, Y. Kaneda, and Y. Kono (2000), Out-of-sequence thrust faults developed in the coseismic slip zone of the 1946 Nankai earthquake (M_w = 8. 2) off Shikoku, southwest Japan, *Geophys. Res. Lett.*, *27*, 1033–1036.

Saffer, D. M., and B. A. Bekins (2002), Hydrologic controls on the morphology and mechanics of accretionary wedges, *Geology*, *30*(3), 271–274.

Taira, A., and M. Tashihiro (1987), Late Paleozoic and Mesozoic accretion tectonics of Japan and eastern Asia, in *Historical Paleogeography and Plate Tectonic Evolution of Japan and Eastern Asia*, edited by A. Taira and M. Tashihiro, pp. 1–47, Terra Publ., Tokyo.

Taira, A., J. Katto, M. Tashiro, M. Okamura, and K. Kodama (1988), The Shimanto Belt in Shikoku, Japan: Evolution of Cretaceous to Miocene accretionary prism, *Mod. Geol.*, *12*, 5–46.

Taira, A., et al. (1991), *Proceedings of the Ocean Drilling Program, Initial Reports*, vol. 131, Ocean Drill. Program, College Station, Tex.

Tamano, T., T. Toba, and Y. Aoki (1983), Development of forearc continental margins and their potential for hydrocarbon accumulation, in *Proceedings of the World Petrology Congress*, pp. 1–11, Portland Press, Colchester, UK.

Yamazaki, T., and Y. Okamura (1989), Subducting seamounts and deformation of overriding forearc wedges around Japan, *Tectonophysics*, *160*, 207–229.

N. L. B. Bangs, S. P. S. Gulick, and T. H. Shipley, University of Texas at Austin, Institute for Geophysics, 4412 Spicewood Springs Road, Bldg. 600, Austin, TX 78759-8500, USA. (nathan@ig.utexas.edu; sean@ig.utexas.edu; tom@ig.utexas.edu)

S. Kuramoto, JAMSTEC, National Institute of Advanced Industrial Science and Technology, Institute for Marine Resources and Environment, 1-1-1 Higashi, Tsukuba, Ibaraki 305-8567, Japan. (s.kuramoto@jamstec.go.jp)

G. Moore, University of Hawaii, Department of Geology and Geophysics, 1680 East-West Road, Post Room 813, Honolulu, HI 96822-2285, USA. (moore@akule.soest.hawaii.edu)

Y. Nakamura, Ocean Research Institute, University of Tokyo, 1-15-1 Minamidai, Nankano, Tokyo 164-8639, Japan. (saru@ori.u-tokyo.ac.jp)